Inorganic Chemistry

Article

pubs.acs.org/IC

Redox Reactions of [FeFe]-Hydrogenase Models Containing an Internal Amine and a Pendant Phosphine

Dehua Zheng,[†] Mei Wang,*[,†] Lin Chen,[†] Ning Wang,[†,‡] and Licheng Sun[†,§]

[†]State Key Laboratory of Fine Chemicals, DUT-KTH Joint Education and Research Center on Molecular Devices, Dalian University of Technology (DUT), Linggong Road 2, Dalian 116024, China

[‡]School of Chemistry and Chemical Engineering, Henan University of Technology, 100 Lianhua Street, Zhengzhou 450001, China

[§]Department of Chemistry, KTH Royal Institute of Technology, Teknikringen 42, Stockholm 10044, Sweden

Supporting Information

ABSTRACT: A diiron dithiolate complex with a pendant phosphine coordinated to one of the iron centers, $[(\mu\text{-}SCH_2)_2N(CH_2C_6H_4\text{-}o\text{-}PPh_2)\{Fe_2(CO)_5\}]$ (**1**), was prepared and structurally characterized. The pendant phosphine is dissociated together with a CO ligand in the presence of excess PMe_3, to afford $[(\mu\text{-}SCH_2)_2N(CH_2C_6H_4\text{-}o\text{-}PPh_2)\{Fe(CO)_2(PMe_3)\}_2]$ (**2**). Redox reactions of **2** and related complexes were studied in detail by in situ IR spectroscopy. A series of new $Fe^{II}Fe^{I}$ ($[\mathbf{3}]^+$ and $[\mathbf{6}]^+$), $Fe^{II}Fe^{II}$ ($[\mathbf{4}]^{2+}$), and $Fe^{I}Fe^{I}$ (**5**) complexes relevant to H_{ox}, H_{ox}^{CO}, and H_{red} states of the [FeFe]-hydrogenase active site were detected. Among these complexes, the molecular structures of the diferrous complex $[\mathbf{4}]^{2+}$ with the internal amine and the pendant phosphine co-coordinated to the same iron center and the triphosphine diiron complex **5** were determined by X-ray crystallography. To make a comparison, the redox reactions of an analogous complex, $[(\mu\text{-}SCH_2)_2N(CH_2C_6H_5)\{Fe(CO)_2(PMe_3)\}_2]$ (**7**), were also investigated by in situ IR spectroscopy in the absence or presence of extrinsic PPh_3, which has no influence on the oxidation reaction of **7**. The pendant phosphine in the second coordination sphere makes the redox reaction of **2** different from that of its analogue **7**.

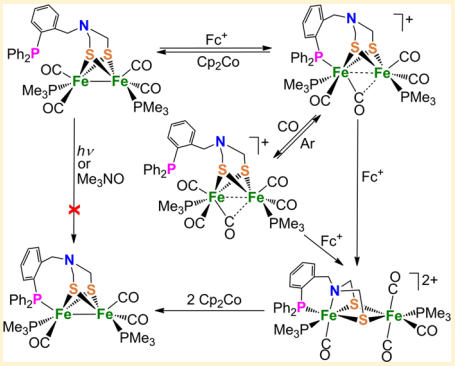

INTRODUCTION

The structural and functional mimicking of the [FeFe]-H_2ase active site and investigation of the enzymatic mechanism for dihydrogen oxidation and proton reduction have been the focus in the fields of organometallic and bioinorganic chemistry since the crystal structure of [FeFe]-hydrogenases ([FeFe]-H_2ases) was unveiled in the end of the most recent century.[1,2] The key structural features of [FeFe]-H_2ase active site are a diiron dithiolate core, an amine cofactor in the S−to−S bridge, and a 4Fe4S cluster tethered to the diiron core through a cysteine residue.[3,4] On the basis of theoretical and experimental studies, different redox states of [FeFe]-H_2ases, namely the super-reduced state (H_{sred}),[5] the reduced state (H_{red}), the oxidized active state (H_{ox}), the CO-inhibited state (H_{ox}^{CO}), and the oxidized inactive state (H_{ox}^{air}), have been proposed for the active site of [FeFe]-H_2ases (Figure 1).[6−8] Studies on the redox properties and reactions of [FeFe]-H_2ase models of these states can give some insights into the mechanism for H_2 evolution and uptake at the [FeFe]-H_2ase active site. The better understanding of enzymatic mechanism will help chemists in designing highly efficient bioinspired catalysts for hydrogen production and oxidation. Over the past decade, numerous synthetic models of H_{red} were reported, and their chemical and electrochemical properties were widely studied.[9−14] Very recently, some $Fe^{I}Fe^{I}$ complexes with a rotated geometry related to the active site of [FeFe]-H_2ase were reported.[15,16] In contrast, reports on the reactivity of [FeFe]-H_2ase models in oxidized states are scarce. To date, only a few structurally characterized mixed-valence diiron models of H_{ox} were reported.[17−22] These models either bear special σ ligands, IMes [1,3-bis(2,4,6-trimethylphenyl)imidazol-2-ylidene],[15] dppv (*cis*-1,2-bis(diphenylphosphino)ethane),[18,19] and dppn (1.8-bis(diphenylphosphino)naphthalene),[20] or feature a bulky bridge, dmpdt (2,2-dimethyl-1,3-propanedithiolate).[21] Recently, a functional model of H_{ox} containing both an internal amine and a redox active unit, FcP* (FcP* = Cp*Fe-($C_5Me_4CH_2PEt_2$), Cp* = C_5Me_5), was reported.[23] Under CO atmosphere, the H_{ox} models readily convert to the corresponding mimics of H_{ox}^{CO} with extrinsic CO coordinating to the vacant apical site at the rotated iron center of H_{ox} models.[24−26]

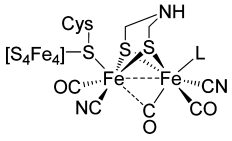

H_{sred}: L = H^+ ($[Fe^{I}Fe^{I}][4Fe4S]^+$)
H_{red}: L = H^+ ($[Fe^{I}Fe^{I}][4Fe4S]^{2+}$)
H_{ox}: L = vacant or H_2O ($[Fe^{II}Fe^{I}][4Fe4S]^{2+}$)
H_{ox}^{CO}: L = CO ($[Fe^{II}Fe^{I}][4Fe4S]^{2+}$)
H_{ox}^{air}: L = H_2O or OH^- ($[Fe^{II}Fe^{II}][4Fe4S]^{2+}$)

Figure 1. H_{sred}, H_{red}, H_{ox}, H_{ox}^{CO}, and H_{ox}^{air} states of the [FeFe]-H_2ase active site.

Received: October 10, 2013
Published: January 14, 2014

dx.doi.org/10.1021/ic4025519 | *Inorg. Chem.* 2014, 53, 1555−1561

Scheme 1. Redox Reactions of 2 and $[3]^+$ in CH_2Cl_2 at −70 °C

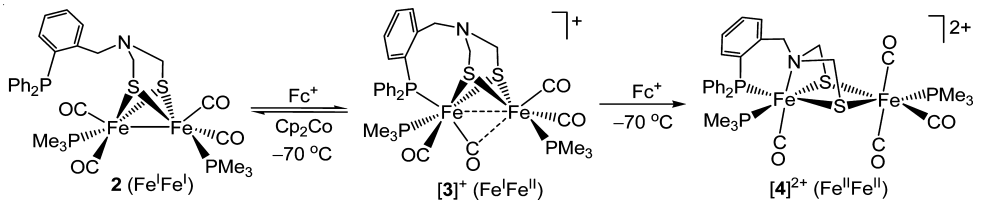

In addition, in situ spectroscopic investigations showed that the one-electron oxidation processes of 2Fe3S models are accompanied by coordination of the pendant thioether group to the rotated iron center.[27,28] Some diferrous dithiolate complexes were also reported as H_{ox}^{air} models of [FeFe]-H_2ases.[24,29−32]

Herein we present a series of redox reactions starting from an [FeFe]-H_2ase model containing an internal amine and a pendant phosphine, $[(\mu\text{-adtP})\{Fe(CO)_2(PMe_3)\}_2]$ (**2**, adtP = $(\mu\text{-}SCH_2)_2NCH_2C_6H_4\text{-}o\text{-}PPh_2$). The two-step one-electron oxidation process of **2** accompanied by intramolecular P- and N-coordination, the reaction of the in situ generated mixed-valence species under CO atmosphere, and the reductions of oxidized $Fe^{II}Fe^{I}$ and $Fe^{II}Fe^{II}$ species were studied by in situ IR spectroscopy. The structures of the diferrous complex $[4]^{2+}$ and its reduced product **5** were determined by crystallographic analyses. These [FeFe]-H_2ase models are interesting because, in $[4]^{2+}$, the internal amine-N atom and the pendant phosphine cocoordinate to the same iron center, and in **5**, there are three donor ligands and three CO ligands like the [FeFe]-H_2ase active site. A comparative study on the redox reaction of an analogous complex $[(\mu\text{-}SCH_2)_2N(CH_2C_6H_4)\{Fe(CO)_2(PMe_3)\}_2]$ (**7**) shows that the pendant phosphine in the second coordination sphere makes the redox property of **2** different from its analogue **7**.

RESULTS AND DISCUSSION

Synthesis and Characterization of 1 and 2. The starting compound, $[(\mu\text{-adtP})Fe_2(CO)_5]$ (**1**), was prepared as a purple powder in 38% yield from the reaction of formaldehyde and 2-$Ph_2PC_6H_4CH_2NH_2$ with a freshly prepared complex $[(\mu\text{-}SH)_2Fe_2(CO)_6]$ in THF.[33] Treatment of **1** with 4 equiv of PMe_3 in refluxing toluene for 6 h afforded a diphosphine complex (**2**) in 48% yield (Scheme 1), together with a byproduct of PMe_3-monosubstituted diiron complex $[(\mu\text{-}SCH_2)_2NCH_2C_6H_4\text{-}o\text{-}PPh_2)\{Fe(CO)_2\}\{Fe(CO)_2(PMe_3)\}]$ (**8**) in ∼28% yield (see the Supporting Information). The crystallographic study (Supporting Information Figure S1, Tables S1−S4), together with ESI-MS (**1**, m/z = 633.8; **8**, 681.9784 for $[M + H]^+$), $^{31}P\{^1H\}$ NMR (**1**, δ = 52.9; **8**, 24.6 and 49.9), and IR (**1**, ν_{CO} = 1928, 1975, 2041 cm^{-1}; **8**, 1909, 1944, 1981 cm^{-1}) spectroscopic data, confirms that the pendant phosphine is coordinated to one of the iron centers in **1** and **8**. In contrast, the $^{31}P\{^1H\}$ NMR spectrum of **2** displays a signal at δ −13.5 for the pendant phosphine in addition to a signal at δ 26.3 for two PMe_3 ligands. This $^{31}P\{^1H\}$ NMR evidence together with MS (m/z = 758.0225 for $[M + H]^+$) and IR (ν_{CO} = 1896, 1941, 1980 cm^{-1}) spectroscopic data of **2** clearly indicates that the CO-displacement of **1** by two PMe_3 ligands leads to dissociations of the pendant phosphine and a CO from the iron centers. A similar association/dissociation of an internal sulfur atom has been previously described for a 2Fe3S complex.[34] Complexes **1** and **2** were also characterized by ^1H and ^{13}C NMR spectroscopy (Supporting Information).

Electrochemistry of 2. The oxidation of **2** was first probed by cyclic voltammetry in a CH_2Cl_2 solution containing 0.1 M Bu_4NPF_6 at −40 °C. The cyclic voltammogram (CV) of **2** displays a quasireversible oxidation event at E_{pa1} = −0.24 V versus $Fc^{+/0}$ for the $Fe^{I}Fe^{I}/Fe^{II}Fe^{I}$ couple and an irreversible oxidation peak at E_{pa2} = −0.02 V versus $Fc^{+/0}$ for the $Fe^{II}Fe^{I}/Fe^{II}Fe^{II}$ process (Figure 2). When the anodic scan returned at −0.16 V to avoid the second oxidation process, the reversibility of the first oxidation event was slightly improved.

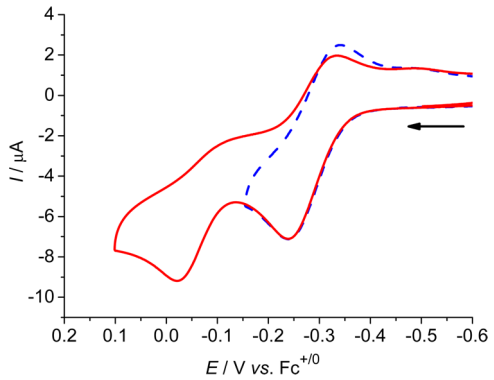

Figure 2. Cyclic voltammograms of **2** (1.0 mM) in 0.1 M Bu_4NPF_6/CH_2Cl_2 at −40 °C with a scan rate of 100 mV s^{-1}.

Chemical Oxidations of 2 and $[3]^+$. Chemical oxidation of **2** was monitored in CH_2Cl_2 by in situ IR spectroscopy at −70 °C (Supporting Information Figure S2a). Upon addition of an equivalent of $FcBAr^F_4$ [Ar^F = 3,5-$(CF_3)_2C_6H_3$], the CO absorptions of **2** shift by 50−80 cm^{-1} to higher energy for its oxidized species $[3]^+$ (ν_{CO} = 1977, 1992, 2036 cm^{-1}), accompanied by appearance of a typical band at 1772 cm^{-1} for a bridging or semibridging CO (Figure 3). Generally, the μ-CO absorptions of $Fe^{II}Fe^{I}$ complexes featuring a vacant apical site at the rotated Fe^{I} center appear in the region of 1830−1940 cm^{-1},[17−21] while the μ-CO bands are observed in the lower energy region of 1770−1800 cm^{-1}, which is typical for $Fe^{II}Fe^{I}$ complexes with the vacant apical site occupied by CO or a pendant donor ligand.[24−26] Noticeably, the IR absorption pattern of $[3]^+$ in the CO absorption region has apparently changed as compared to that of its parent complex **2**, implicating a considerable change in the symmetry of the molecule. Taking into account this IR evidence, we assume that the one-electron oxidation of **2** concurs with coordination of the pendant phosphine (Scheme 1), as observed for the one-electron oxidation of diiron complexes bearing a pendant thioether group.[27,28] The mixed-valence complex $[3]^+$ is only stable in CH_2Cl_2 below −50 °C. The characteristic CO absorptions of **2** were quantitatively recovered when an equivalent of Cp_2Co was added to the CH_2Cl_2 solution of

dx.doi.org/10.1021/ic4025519 | Inorg. Chem. 2014, 53, 1555−1561

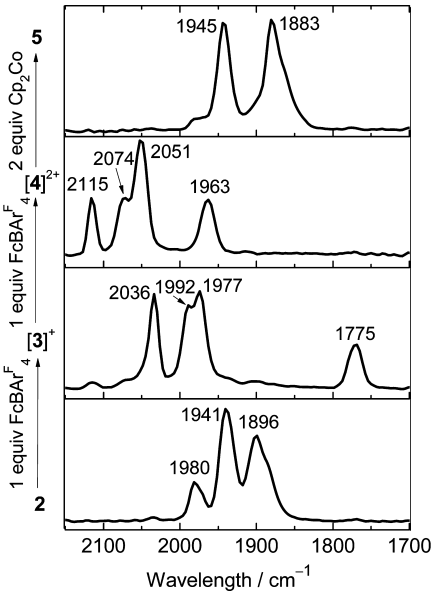

Figure 3. IR spectra of **2**, $[3]^+$, $[4]^{2+}$, and **5** in CH_2Cl_2 at −70 °C.

$[3]^+$ at −70 °C, indicative of a good chemical reversibility of redox reactions between **2** and $[3]^+$ at low temperature (Supporting Information Figure S2b).

The irreversibility of the second oxidation event of **2** in CV implies that some irreversible chemical reaction occurs rapidly following the oxidation reaction. The chemical oxidation of $[3]^+$, in situ generated by oxidation of **2** with 1 equiv of $FcBAr^F{}_4$ in CH_2Cl_2 at −70 °C, was monitored by in situ IR spectroscopy (Supporting Information Figure 2Sa). Upon addition of an extra equivalent of $FcBAr^F{}_4$, the absorptions of terminal CO ligands of $[3]^+$ immediately shift by ∼80 cm^{-1} to higher energy, and no band is observed in the bridging CO absorption region 1770−1940 cm^{-1} (Figure 3). The $^{31}P\{^1H\}$ NMR spectrum of the diferrous complex ($[4]^{2+}$) displays three $^{31}P\{^1H\}$ NMR signals at δ 11.21 (d, J_{pp} = 38.15 Hz, PMe_3), 15.79 (s, PMe_3), and 54.20 (d, J_{pp} = 38.15 Hz, PPh_2Ar, Ar = C_6H_4-*o*-$CH_2N(CH_2S$-$\mu)_2$), indicating an unsymmetrical structure of $[4]^{2+}$. Accordingly, the hydrogen atoms of three CH_2 groups in $[4]^{2+}$ exhibit two doublets at δ 6.11, 6.32 (2H, CH_2Ar) and two doublets of doublets at δ 4.71, 5.48 [4H, $N(CH_2S)_2$], while two singlets are observed for these CH_2 groups in **1** (δ 3.07 (4H), 4.22 (2H)) and **2** (δ 3.19 (4H), 4.19 (2H)). The NMR spectroscopic evidence suggests the coordination of the internal amine-N atom to one of the iron centers of $[4]^{2+}$.

Chemical Reduction of $[4]^{2+}$. Treatment of $[4]^{2+}$ with 2 equiv of Cp_2Co in CH_2Cl_2 at −70 °C leads to dramatic shifts of CO absorptions to 1945 and 1882 cm^{-1} for the reduced Fe^IFe^I complex (**5**) with an apparent change in IR CO absorption pattern (Figure 3 and Supporting Information Figure S3). Complex **5** displays three $^{31}P\{^1H\}$ NMR singlets at δ 17.42, 21.18, and 60.90, indicating that the pendant phosphine is still coordinated to the iron center. The specialty of **5** is that it has three donor ligands and three CO ligands like the [FeFe]-H_2ase active site. Although a number of diphosphine-substituted diiron dithiolate complexes have been reported, only a few trisphosphine diiron complexes were found in the literature because of difficulty in the further CO-displacement of diphosphine complexes.[19,23,35,36] For example, complex **5** cannot be obtained either by treatment of **1** with 4 equiv of PMe_3 in refluxing toluene, or by direct treatment of the toluene solution of **2** in the presence of Me_3NO or under irradiation of light (Scheme 2).

Scheme 2. Substitution and Redox Reactions of 1, 2, and $[4]^{2+}$

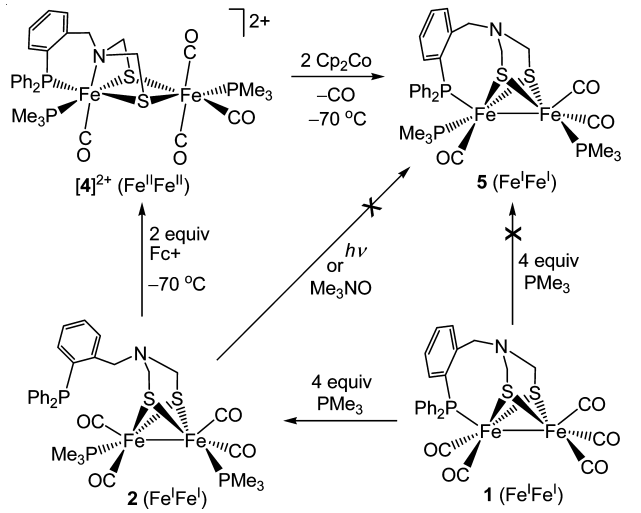

Molecular Structures of $[4]^{2+}$ and 5. X-ray crystallographic analysis of $[4]^{2+}$ demonstrates that the pendant phosphine and internal amine are co-coordinated to the same iron center with the S−Fe−N angles of 73.95(10)° and the N−Fe(1)−P(1) angle of 90.67(11)° (Figure 4, Supporting Information Tables S1 and S2). This iron center features a six-coordinate distorted octahedral geometry, in which a PMe_3 and pendant phosphine together with two thiolates are *cis*-coordinated to the iron center in a square plane with the coordinated internal N atom and a CO ligand in the two apexes of octahedron. The other iron center is coordinated in a nearly standard octahedral geometry by two thiolates, a PMe_3 and three CO ligands in a meridional configuration. The long Fe···Fe distance of 3.5174(12) Å indicates that the two Fe^{II} ions are nonbonding but still linked by two thiolates. The spectroscopic and crystallographic results show that the oxidation of $[3]^+$ is accompanied by coordination of the internal amine to the rotated iron center and by transfer of the semibridging CO from the rotated iron center to the nonrotated one. The structure of $[4]^{2+}$ is uncommon. To our knowledge, only one example was reported to date on the [FeFe]-H_2ase model with an internal amine-N atom of the S-to-S bridge coordinated to an iron center.[32]

Single crystal X-ray analysis of **5** (Figure 4, Supporting Information Tables S1 and S2) shows that one of the CO ligands is lost and the internal amine is dissociated from the iron center, resulting in the reformation of an Fe−Fe bond with a bond length (2.5861(4) Å) close to that (2.6 Å) for the [FeFe]-H_2ase active site.[37] Complex **5** has a similar butterfly conformation as previously reported diiron dithiolato complexes.[38,39] The angle of P(2)−Fe(1)−Fe(2) (102.30(2)°) is apparently smaller than that of P(3)−Fe(2)−Fe(1) (109.19(2)°) because of the bulkiness of pendant phosphine ligand.

Comparative Study on the Redox Reaction of 7. Complex **7**, $[(\mu$-$SCH_2)_2NCH_2C_6H_4\}\{Fe(CO)_2(PMe_3)\}_2]$, is a well-known diiron complex, and it was prepared as a reference compound according to the literature procedure.[40] To

dx.doi.org/10.1021/ic4025519 | Inorg. Chem. 2014, 53, 1555−1561

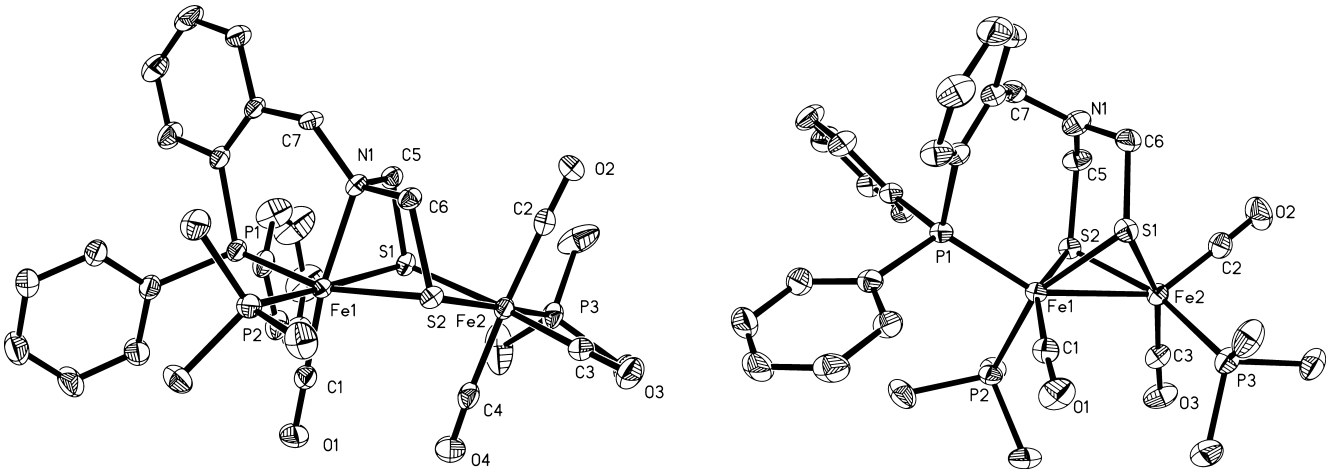

Figure 4. Molecular structures of $[4]^{2+}$ (left) and **5** (right) with thermal ellipsoids set at 30% level. Hydrogen atoms were omitted for clarity. Selected bond lengths (Å) and angles (deg) for $[4]^{2+}$: Fe(1)−Fe(2), 3.5174(12); Fe(1)−N(1), 2.037(4); Fe(1)−P(1), 2.250(13); Fe(1)−P(2), 2.2891(15); Fe(2)−P(3), 2.2725(16); Fe(1)−S_{av}, 2.3660; Fe(2)−S_{av}, 2.3165; Fe(1)−C(1), 1.749(5); Fe(2)−C_{av}, 1.826; N(1)−Fe(1)−P(1), 90.67(11); C(1)−Fe(1)−S(2), 101.32(17); N(1)−Fe(1)−S(2), 73.95(10); P(1)−Fe(1)−S(1), 92.16(5); S−Fe−S_{av}, 79.94; C(2)−Fe(2)−C(4), 175.6(2). For **5**: Fe(1)−Fe(2), 2.5862(4); Fe−S_{av}, 2.2637; Fe(1)−P(1), 2.2505(6); Fe−$P(PMe_3)_{av}$, 2.2353; Fe(1)−C(1), 1.731(2); Fe(2)−C_{av}, 1.7635; P(1)−Fe(1)−S(2), 106.45(2); P(2)−Fe(1)−Fe(2), 102.30(2); P(1)−Fe(1)−Fe(2), 149.945(19); P(2)−Fe(1)−P(1), 101.32(2).

Scheme 3. Redox Reactions of 7 at −70 °C

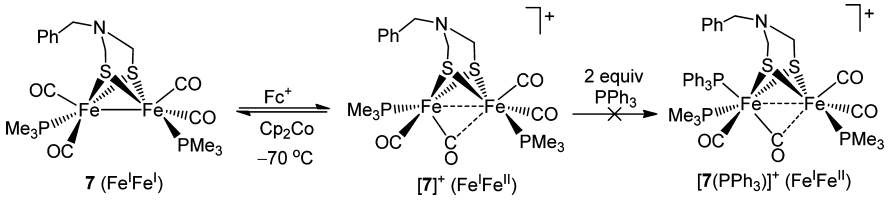

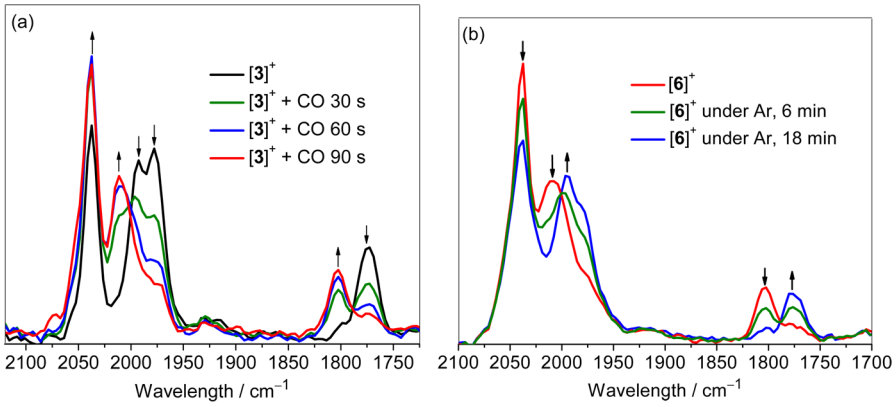

Figure 5. IR spectra monitoring (a) the reaction of $[3]^+$ with CO over a period of 90 s and (b) the process of the back reaction of $[6]^+$ to $[3]^+$ over a period of 18 min in CH_2Cl_2 at −70 °C under Ar.

understand the influence of a pendant phosphine in the second coordination sphere, the oxidation reactions of **7**, an analogue of **2**, were also studied in the absence and presence of extrinsic PPh_3. Similar to **2**, complex **7** also displays a quasireversible oxidation event for the $Fe^IFe^I/Fe^{II}Fe^I$ couple (E_{pa1} = −0.16 V vs $Fc^{+/0}$) and an irreversible oxidation peak for the $Fe^{II}Fe^I/Fe^{II}Fe^{II}$ process (E_{pa2} = +0.08 V vs $Fc^{+/0}$, Supporting Information Figure S4) at potentials 80−100 mV more positive than those of **2** in 0.1 M Bu_4NPF_6/CH_2Cl_2.

The in situ IR monitoring shows that, upon addition of an equivalent of $FcBAr^F{}_4$, the CO absorptions of **7** at 1985, 1948, and 1908 cm^{-1} disappeared within 2 min at −70 °C in CH_2Cl_2, accompanied with appearance of three new CO bands at 2045, 2007, and 1866 cm^{-1} (Supporting Information Figure S5a) regardless of absence or presence of PPh_3. The last band with lowest energy is attributed to the absorption of a μ-CO ligand in the one-electron oxidized species $[7]^+$. Upon addition of PPh_3 to the CH_2Cl_2 solution of $[7]^+$, no change was observed in the in situ IR spectra, implicating that the extrinsic PPh_3 cannot coordinate to the iron center of the rotated $Fe(CO)_2(PMe_3)$ unit (Scheme 3). The oxidative coordination reactivity of **7** with two identical units, $Fe(CO)_2(PMe_3)$, linked by a dithiolate bridge is different from diiron dithiolate complexes containing an unsymmetrical chelating ligand. It is reported that (μ-pdt){Fe(CO)(L^L)}{Fe(CO)$_3$} (L^L = 1,2-bis(diphenylphosphino)ethane (dppe), I_{Me}-CH_2−I_{Me}, I_{Me} = 1-

dx.doi.org/10.1021/ic4025519 | Inorg. Chem. 2014, 53, 1555−1561

methylimidazol-2-ylidene) complexes are readily coordinated by an extrinsic phosphite ligand at the rotated $Fe(CO)_3$ unit after one-electron oxidation,[41,42] most possibly due to less electron density and steric hindrance of the Fe center in the rotated $Fe(CO)_3$ unit of (μ-pdt){Fe(CO)(L^L)}{$Fe(CO)_3$} as compared to the $Fe(CO)_2(PMe_3)$ moiety of $[7]^+$. The large difference in the μ-CO bands, $\nu_{\mu\text{-CO}}$ = 1772 cm^{-1} for $[3]^+$ and 1866 cm^{-1} for $[7]^+$, gives further support for the coordination of the pendant phosphine during the oxidation process of **2** to $[3]^+$, while an extrinsic PPh_3 is not involved in the one-electron oxidation reaction of **7**. The oxidized species $[7]^+$ returns to **7** immediately upon addition of an equivalent of Cp_2Co (Supporting Information Figure S5b). In situ IR monitoring also shows that further oxidation of $[7]^+$ by $FcBAr^F{}_4$, even in an excess (up to 4 equiv), is difficult due to the small driving force considering the potentials for the second oxidation of **7** and the reduction of Fc^+ to Fc.

Reaction of $[3]^+$ with CO and Chemical Oxidation of $[6]^+$. It is reported that the mixed-valence diiron models readily take up extrinsic CO to the open site of the rotated Fe^I center.[24−26] Although there is no vacant coordination site in $[3]^+$, upon bubbling of CO into the CH_2Cl_2 solution of $[3]^+$ at −70 °C, the CO absorptions of $[3]^+$ disappeared within 2 min (Figure 5a). The most noticeable change is the semibridging CO absorptions, shifting from 1770 to 1800 cm^{-1} (Supporting Information Figure S6). The terminal CO bands at 1990 and 1975 cm^{-1} for $[3]^+$ merge into one band, which shifts to 2011 cm^{-1} for the resulting complex ($[6]^+$), while the position of the highest energy CO stretch of $[3]^+$ at 2037 cm^{-1} remains unchanged but the intensity of this band appears to increase relative to the other CO bands. On the basis of the changes in IR spectra, we assume that the coordinated pendant phosphine at the open site of the rotated Fe^I center is replaced by extrinsic CO to form a product of symmetric structure containing two $Fe(CO)_2PMe_3$ units linked by a pair of thiolatos and a μ-CO ligand (Scheme 4). The shift of the CO bands to higher wavenumbers is due to the better π-acceptor ability of CO ligand as compared to PPh_3. The easy displacement of the coordinated pendant phosphine by CO in the formation of $[6]^+$ from $[3]^+$ and by PMe_3 in the preparation of **2** from **1** shows that the coordination of the pendant phosphine in the mixed-valence diiron complex $[3]^+$ is quite labile. When the inert gas (Ar) was bubbled into the solution of $[6]^+$ at −70 °C, the four CO absorptions of $[3]^+$ was completely recovered in about 20 min (Figure 5b), indicating that the extra CO in $[6]^+$ can be readily replaced by the pendant phosphine under Ar to regenerate $[3]^+$.

Moreover, the purple solution of $[6]^+$ immediately changed to reddish yellow upon addition of an equivalent of $FcBAr^F{}_4$. The resulting solution gives an exactly identical IR spectrum to that of $[4]^{2+}$, indicating that during the further one-electron oxidation process of $[6]^+$ the coordination of both the internal amine and the pendant phosphine to the same iron center occurs, accompanied by loss of a CO and transformation of the semibridging CO to a terminal CO (Supporting Information Figure S7).

Scheme 4. Redox Reactions of $[3]^+$, $[4]^{2+}$, and $[6]^+$ at −70 °C

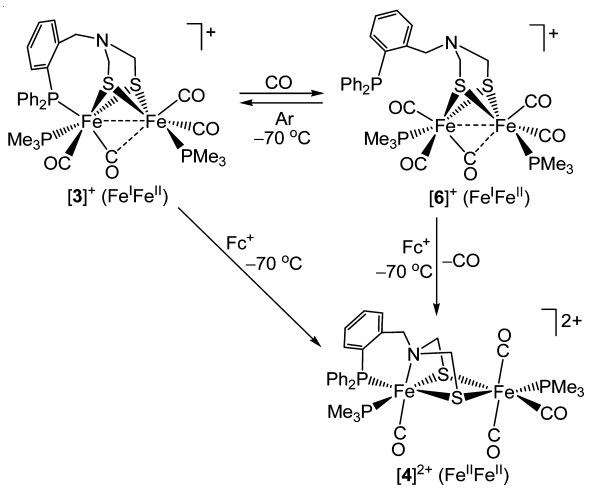

CONCLUSIONS

Redox reactions of **2**, $[3]^+$, $[4]^{2+}$, and $[6]^+$ are all accompanied by association/dissociation of the pendant phosphine ligand and/or internal amine. The coordinated pendant phosphine is readily replaced by extrinsic CO and PMe_3. The facile association/dissociation of the internal amine implicates that the central N atom of S-to-S bridge can function not only as a proton transfer relay in the process of proton reduction to hydrogen, but also as an electron donor to stabilize the coordination-unsaturated Fe^{II} center in the oxidation reaction of [FeFe]-H_2ase models. The flexibility of 2Fe2S framework is evinced by reversible conversion of 2Fe2S core between a butterfly and quasisquare configuration in the oxidation process of $[3]^+$ to $[4]^{2+}$ and the reduction process of $[4]^{2+}$ to **5**. Successive oxidative/reductive CO-displacement of diphosphine complex **2** in one pot affords a triphosphine Fe^IFe^I complex **5** in good yield, which cannot be prepared by direct CO-displacement of **1** and **2**. Comparative studies on the oxidation of **7** in the absence and presence of PPh_3 show that the effect of the pendant phosphine in the second coordination sphere on the stability of oxidized species of [FeFe]-H_2ase models cannot be surrogated by an extrinsic phosphine ligand.

EXPERIMENTAL SECTION

Reagents and Instruments. All reactions and operations related to organometallic compounds were carried out under dry, oxygen-free dinitrogen atmosphere with standard Schlenk techniques. Solvents were dried and distilled prior to use according to the standard methods. The reagents $LiEt_3BH$ and 3,5-bis(trifluoromethyl)-bromobenzene were purchased from Aldrich. Other commercially available chemicals such as $Fe(CO)_5$, Cp_2Fe, Cp_2Co, trifluoroacetic acid, and 36% formalin were purchased from local suppliers and used as received. Compounds $[(\mu\text{-}S_2)Fe_2(CO)_6]$,[43] **7**,[40] (2-(diphenylphosphino)phenyl)methylamine,[44] and $FcBAr^F{}_4$[45] were prepared according to literature procedures.

Infrared spectra were measured with a JASCO FT/IR 430 spectrophotometer. In situ IR spectra were recorded using a Mettler-Toledo ReactIR 15 System equipped with an MCT detector and a Dsub AgX SiComp in situ probe. ^1H and $^{31}P\{^1H\}$ NMR spectra were collected with a Varian INOVA 400 NMR spectrometer. Mass spectra were recorded either on a TOF mass spectrometer (Micromass) or an Agilent 6224 Accurate-Mass TOF mass spectrometer.

Preparation of 1. To a red solution of $[(\mu\text{-}S_2)Fe_2(CO)_6]$ (2.0 g, 5.81 mmol) in THF (30 mL) at −78 °C was added 12 mL of a 1.0 M $LiEt_3BH$ (12.0 mmol). The resulting green solution was allowed to stir for another 2 h, followed by dropwise addition of trifluoroacetic acid (1.0 mL). After the solution was allowed to warm to room temperature, a portion of a 36% formalin solution (1.0 mL, 12.0 mmol) was added, and the solution was stirred for 1 h. Compound [2-

dx.doi.org/10.1021/ic4025519 | Inorg. Chem. 2014, 53, 1555−1561

(diphenylphosphino)phenyl]methylamine (1.69 g, 5.83 mmol) was then added, and the mixture was stirred at 60 °C overnight. The solvent was then removed on a rotary evaporator. The crude product was purified by chromatography on silica gel first with CH_2Cl_2 and then with petroleum ether as eluents. Product **1** was isolated as a purple powder in 38% yield (1.4 g) after the solvent was removed under reduced pressure. Crystals of **1** were obtained from CH_2Cl_2/hexane at room temperature. IR (CH_2Cl_2): ν_{CO} = 1928, 1975, 2041 cm^{-1}. ^1H NMR ($CDCl_3$): δ = 3.07 (s, 4H, $N(CH_2S)_2$), 4.22 (s br, 2H, NCH_2Ar), 7.06, 7.30, 7.41, 7.61 (4t, 4H), and 7.49 (s br, 10H) for Ph and Ar. ^{13}C NMR ($CDCl_3$): δ 209.1, 207.9, 141.4, 138.8, 133.4, 132.2, 130.7, 128.8, 127.9, 55.3, 51.7. $^{31}P\{^1H\}$ NMR ($CDCl_3$): δ = 52.9 (s, PPh_2Ar). ESI-MS: found for $[M + H]^+$, m/z 633.8; for $[M + Na]^+$, 655.8; calcd for $[\mathbf{1}]^+$, m/z 632.9. Anal. Calcd for $C_{26}H_{20}NO_5S_2PFe_2$: C, 49.31; H, 3.18; N, 2.21%. Found: C, 49.18; H, 3.17; N, 2.19%.

Preparation of 2. To a purple solution of **1** (0.16 g, 0.25 mmol) in toluene (50 mL) was added a PMe_3 hexane solution (0.11 mL, 1.0 mmol, 9.7 M). After the resulting solution was refluxed for 6 h, the solvent was removed on a rotary evaporator. The crude product was purified by chromatography on silica gel with hexane/CH_2Cl_2 (2:1, v/v) as eluent. The first red band afforded **2** in 48% yield (91 mg). The second band contained mainly the PMe_3-monosubstituted diiron complex **8** (yield: ~28%, 50 mg), which was always contaminated with **2** as these mono- and disubstituted diiron complexes have very similar polarity and solubility.

Characterization data for **2** follow. IR (CH_2Cl_2): ν_{CO} = 1896, 1941, 1980 cm^{-1}. ^1H NMR ($CDCl_3$): δ = 1.46 and 1.48 (2s, 18H, $P(CH_3)_3$), 3.19 (s, 4H, $N(CH_2S)_2$), 4.19 (s, 2H, NCH_2Ar), 6.85, 7.14, 7.30, and 7.45 (4s br, 14H, Ph and Ar). ^{13}C NMR (THF-d_8): 207.9, 141.1, 138.0, 133.6, 131.3, 129.8, 128.2, 127.3, 58.4, 51.7, 19.2, 18.9. $^{31}P\{^1H\}$ NMR ($CDCl_3$): δ = 26.3 (s, 2PMe_3), −13.5 (s, PPh_2Ar). HR-ESI-MS: found for $[M + H]^+$, m/z 758.0225; calcd for **2**, 757.0154. Anal. Calcd for $C_{31}H_{38}NO_4S_2P_3Fe_2$: C, 49.16; H, 5.06; N, 1.85%. Found: C, 48.92; H, 5.09; N, 1.84%.

Characterization data for **8** follow. IR (CH_2Cl_2): ν_{CO} = 1909, 1944, 1981 cm^{-1}. ^1H NMR ($CDCl_3$): δ = 1.47 (s, 9H, $P(CH_3)_3$), 3.25 (s, 4H, NCH_2S), 3.40 (s, 2H, NCH_2Ar), 6.99, 7.22, 7.30, 7.50 (4s br, 14H, Ph and Ar). $^{31}P\{^1H\}$ NMR ($CDCl_3$): δ = 24.6 (s, 1P, PMe_3), 49.9 (s, 1P, PPh_2Ar). HR-ESI-MS: calcd for $C_{28}H_{29}NO_4S_2P_2Fe_2$, m/z 680.9712; found for $[M + H]^+$, m/z 681.9784. Anal. Calcd for $C_{28}H_{29}NO_4S_2P_2Fe_2$: C, 49.36; H, 4.29; N, 2.06%. Found: C, 48.98; H, 4.26; N, 2.05%.

Preparation of $[4]^{2+}$. Complex **2** (0.03 g, 0.04 mmol) was dissolved in CH_2Cl_2 (3 mL), and the solution was cooled to −70 °C under Ar. The precooled solution of $FcBAr^F_4$ (83.2 mg, 0.08 mmol) in CH_2Cl_2 (3 mL) was transferred to the above solution. After the mixture was stirred at −70 °C for 0.5 h, the precooled hexane (10 mL) was added to precipitate the product, which was collected by filtration. The reddish brown crude product was washed with 2 × 2.5 mL pentane to further remove impurities. Complex $[4]^{2+}$ was obtained in 92% yield (92 mg). Crystals suitable for single crystal analysis was obtained by recrystallization of $[4]^{2+}$ from CH_2Cl_2/hexane at 4 °C. IR (CH_2Cl_2): ν_{CO} = 2115, 2074, 2051, 1963 cm^{-1}. ^1H NMR ($CDCl_3$): δ = 1.80 and 1.83 [2s, 18H, $P(CH_3)_3$], 4.67 and 4.76 [2d, J_{HH} = 16.8 Hz, 2H, $N(CH_2S)_2$], 5.44 and 5.52 [2d, J_{HH} = 13.2 Hz, 2H, $N(CH_2S)_2$], 6.11 and 6.32 (2d, J_{HH} = 12.6 Hz, 2H, NCH_2Ar), 7.15, 7.22, 7.61, and 7.85 (4s br, 14H, Ph and Ar). $^{31}P\{^1H\}$ NMR ($CDCl_3$): δ = 11.21 (d, J_{pp} = 38.15 Hz, PMe_3), 15.79 (s, PMe_3), 54.20 (d, J_{pp} = 38.15 Hz, PPh_2Ar). ESI-MS (m/z): found, 378.0 for $[M]^{2+}$; calcd for $[4]^{2+}$, 378.5.

Preparation of 5. Complex $[4](BAr^F_4)_2$ (198.8 mg, 0.08 mmol) was dissolved in CH_2Cl_2 (5 mL), and the solution was cooled to −70 °C under Ar. The precooled solution of Cp_2Co (30.4 mg, 0.16 mmol) in CH_2Cl_2 (5 mL) was transferred to the above solution. After the mixture was stirred at −70 °C for 0.5 h, the solvent was removed under reduced pressure, and the residue was extracted with CH_2Cl_2/hexane (1:3, v/v). Complex **5** was obtained in 52% yield (30 mg). Crystals suitable for single crystal analysis was obtained by recrystallization of **5** from CH_2Cl_2/hexane at room temperature. IR (CH_2Cl_2): ν_{CO} = 1945, 1883 cm^{-1}. ^1H NMR ($CDCl_3$): δ = 1.25 and 1.37 [2s, 18H, $P(CH_3)_3$], 3.40 [s br, 4H, $N(CH_2S)_2$], 4.11 (s, 2H, NCH_2Ar), 6.90−7.95 (br, 14H, Ph and Ar). $^{31}P\{^1H\}$ NMR ($CDCl_3$): δ = 17.42 (s, PMe_3), 21.18 (s, PMe_3), 60.90 (s, PPh_2Ar). HR-ESI-MS (m/z): found, 730.0266 for $[M + H]^+$; calcd for **5**, 729.0205. Anal. Calcd for $C_{30}H_{38}NO_3S_2P_3Fe_2$: C, 49.40; H, 5.25; N, 1.92%. Found: C, 49.05; H, 5.22; N, 1.89%.

X-ray Structure Determination of 1, $[4](BAr^F_4)_2$, and 5. The single-crystal X-ray diffraction data were collected with an Bruker Smart Apex II CCD diffractometer with graphite-monochromated Mo Kα radiation (λ = 0.0710 73 Å) using the $\omega-2\theta$ scan mode. Data processing was accomplished with the SAINT processing program.[46] Intensity data were corrected for absorption by the SADABS program.[47] All structures were solved by direct methods and refined on F^2 against full-matrix least-squares methods by using the SHELXTL 97 program package.[48] All non-hydrogen atoms were refined anisotropically. Hydrogen atoms were located by geometrical calculation. Details of crystal data, data collections, and structure refinements are summarized in Supporting Information Table S1, and selected bond lengths and bond angles are listed in Supporting Information Table S2. CCDC-953860 (**1**), -953859 ($[4](BAr^F_4)_2$), and -953861 (**5**) contain the supplementary crystallographic data for this Article. These data can be obtained free of charge from The Cambridge Crystallographic Data Centre via www.ccdc.cam.ac.uk/data_request/cif.

Electrochemistry Measurements of 2 and 7. Cyclic voltammograms were recorded in a three-electrode cell under Ar using CHI 630D electrochemical workstation. The working electrode was a glassy carbon disc (diameter 3 mm) polished with 3 and 1 μm diamond pastes and sonicated in ion-free water for 15 min prior to use. The reference electrode was a nonaqueous Ag^+/Ag (0.01 M $AgNO_3$ in CH_3CN) electrode, and the counter electrode was platinum wire. A solution of 0.1 M nBu_4NPF_6 (Fluka, electrochemical grade) in CH_2Cl_2 was used as supporting electrolyte, which was degassed by bubbling with dry argon for 15 min before measurement. The ferricinium/ferrocene (Fc^+/Fc) couple was used as an internal reference, and all potentials given in this work are referred to the $Fc^{+/0}$ potential.

■ ASSOCIATED CONTENT

Ⓢ Supporting Information

Cyclic voltammogram of **7**; in situ IR spectra for the redox reactions of **2**, $[4]^{2+}$, $[6]^+$, and **7**, and for the reaction of $[3]^+$ with CO; crystallographic data of **1**, $[4](BAr^F_4)_2$, **5**, and **8**; crystal structures of **1** and **8**. Crystallographic data in CIF format. This material is available free of charge via the Internet at http://pubs.acs.org.

■ AUTHOR INFORMATION

Corresponding Author

*E-mail: symbueno@dlut.edu.cn.

Notes

The authors declare no competing financial interest.

■ ACKNOWLEDGMENTS

We are grateful to the Natural Science Foundation of China (Grants 21373040, 21120102036, and 21101057), the Basic Research Program of China (Grant 2014CB239402), the Swedish Energy Agency, and the K & A Wallenberg Foundation for financial support of this work.

■ REFERENCES

(1) Nicolet, Y.; Lemon, B. J.; Fontecilla-Camps, J. C.; Peters, J. W. *Trends Biochem. Sci.* **2000**, *25*, 138−143.

(2) Fontecilla-Camps, J. C.; Amara, P.; Cavazza, C.; Nicolet, Y.; Volbeda, A. *Nature* **2009**, *460*, 814−822.

(3) Nicolet, Y.; De Lacey, A. L.; Vernéde, X.; Fernandez, V. M.; Hatchikian, E. C.; Fontecilla-Camps, J. C. *J. Am. Chem. Soc.* **2001**, *123*, 1596−1601.
(4) Fontecilla-Camps, J. C.; Volbeda, A.; Cavazza, C.; Nicolet, Y. *Chem. Rev.* **2007**, *107*, 4273−4303.
(5) Adamska, A.; Silakov, A.; Lambertz, C.; Ruediger, O.; Happe, T.; Reijerse, E.; Lubitz, W. *Angew. Chem., Int. Ed.* **2012**, *51*, 11458−11462.
(6) Chen, Z.; Lemon, B. J.; Huang, S.; Swartz, D. J.; Peters, J. W.; Bagley, K. A. *Biochemistry* **2002**, *41*, 2036−2043.
(7) Liu, Z.-P.; Hu, P. *J. Am. Chem. Soc.* **2002**, *124*, 5175−5182.
(8) Capon, J.-F.; Gloaguen, F.; Pétillon, F. Y.; Schollhammer, P.; Talarmin, J. *Coord. Chem. Rev.* **2009**, *253*, 1476−1494.
(9) Capon, J.-F.; Gloaguen, F.; Schollhammer, P.; Talarmin, J. *Coord. Chem. Rev.* **2005**, *249*, 1664−1676.
(10) Liu, X.; Ibrahim, S. K.; Tard, C.; Pickett, C. J. *Coord. Chem. Rev.* **2005**, *249*, 1641−1652.
(11) Felton, G. A. N.; Mebi, C. A.; Petro, B. J.; Vannucci, A. K.; Evans, D. H.; Glass, R. S.; Lichtenberger, D. L. *J. Organomet. Chem.* **2009**, *694*, 2681−2699.
(12) Tard, C.; Pickett, C. J. *Chem. Rev.* **2009**, *109*, 2245−2274.
(13) Heinekey, D. M. *J. Organomet. Chem.* **2009**, *694*, 2671−2680.
(14) Tschierlei, S.; Ott, S.; Lomoth, R. *Energy Environ. Sci.* **2011**, *4*, 2340−2352.
(15) Munery, S.; Capon, J.-F.; De Gioia, L.; Elleouet, C.; Greco, C.; Petillon, F. Y.; Schollhammer, P.; Talarmin, J.; Zampella, G. *Chem.—Eur. J.* **2013**, *19*, 15458−15461.
(16) Wang, W.; Rauchfuss, T. B.; Moore, C. E.; Rheingold, A. L.; De Gioia, L.; Zampella, G. *Chem.—Eur. J.* **2013**, *19*, 15476−15479.
(17) Liu, T.; Darensbourg, M. Y. *J. Am. Chem. Soc.* **2007**, *129*, 7008−7009.
(18) Justice, A. K.; Rauchfuss, T. B.; Wilson, S. R. *Angew. Chem., Int. Ed.* **2007**, *46*, 6152−6154.
(19) Justice, A. K.; Gioia, L. D.; Nilges, M. J.; Rauchfuss, T. B.; Wilson, S. R.; Zampella, G. *Inorg. Chem.* **2008**, *47*, 7405−7414.
(20) Camara, J. M.; Rauchfuss, T. B. *J. Am. Chem. Soc.* **2011**, *133*, 8098−8101.
(21) Singleton, M. L.; Bhuvanesh, N.; Reibenspies, J. H.; Darensbourg, M. Y. *Angew. Chem., Int. Ed.* **2008**, *47*, 9492−9495.
(22) Gloaguen, F.; Rauchfuss, T. B. *Chem. Soc. Rev.* **2009**, *38*, 100−108.
(23) Camara, J. M.; Rauchfuss, T. B. *Nat. Chem.* **2012**, *4*, 26−30.
(24) Justice, A. K.; Nilges, M. J.; Rauchfuss, T. B.; Wilson, S. R.; Gioia, L. D.; Zampella, G. *J. Am. Chem. Soc.* **2008**, *130*, 5293−5301.
(25) Thomas, C. M.; Liu, T.; Hall, M. B.; Darensbourg, M. Y. *Inorg. Chem.* **2008**, *47*, 7009−7024.
(26) Thomas, C. M.; Liu, T.; Hall, M. B.; Darensbourg, M. Y. *Chem. Commun.* **2008**, 1563−1565.
(27) Razavet, M.; Borg, S. J.; George, S. J.; Best, S. P.; Fairhurst, S. A.; Pickett, C. J. *Chem. Commun.* **2002**, 700−701.
(28) Erdem, Ö. F.; Schwartz, L.; Stein, M.; Silakov, A.; Kaur-Ghumaan, S.; Huang, P.; Ott, S.; Reijerse, E. J.; Lubitz, W. *Angew. Chem., Int. Ed.* **2011**, *50*, 1439−1443.
(29) Boyke, C. A.; Rauchfuss, T. B.; Wilson, S. R.; Rohmer, M.-M.; Bénard, M. *J. Am. Chem. Soc.* **2004**, *126*, 15151−15160.
(30) Boyke, C. A.; Vlugt, J. I.; Rauchfuss, T. B.; Wilson, S. R.; Zampella, G.; Gioia, L. D. *J. Am. Chem. Soc.* **2005**, *127*, 11010−11018.
(31) Vlugt, J. I.; Rauchfuss, T. B.; Wilson, S. R. *Chem.—Eur. J.* **2006**, *12*, 90−98.
(32) Olsen, M. T.; Rauchfuss, T. B.; Wilson, S. R. *J. Am. Chem. Soc.* **2010**, *132*, 17733−17740.
(33) Seyferth, D.; Womack, G. B.; Henderson, R. S. *Organometallics* **1986**, *5*, 1568−1575.
(34) Daraosheh, A. Q.; Harb, M. K.; Windhager, J.; Goerls, H.; El-khateeb, M.; Weigand, W. *Organometallics* **2009**, *28*, 6275−6280.
(35) Justice, A. K.; Zampella, G.; Gioia, L. D.; Rauchfuss, T. B.; Vlugt, J. I.; Wilson, S. R. *Inorg. Chem.* **2007**, *46*, 1655−1664.
(36) Olsen, M. T.; Barton, B. E.; Rauchfuss, T. B. *Inorg. Chem.* **2009**, *48*, 7507−7509.
(37) Peters, J. W.; Lanzilotta, W. N.; Lemon, B. J.; Seefeldt, L. C. *Science* **1998**, *282*, 1853−1858.
(38) Cabeza, J. A.; Martínez-Carcía, M. A.; Riera, V. *Organometallics* **1998**, *17*, 1471−1477.
(39) Hasan, M. M.; Hursthouse, M. B.; Kabir, S. E.; Malik, K. M. A. *Polyhydron* **2001**, *20*, 97−101.
(40) Schwartz, L.; Eilers, G.; Eriksson, L.; Gogoll, A.; Lomoth, R.; Ott, S. *Chem. Commun.* **2006**, 520−522.
(41) Chouffai, D.; Zampella, G.; Capon, J.-F.; De Gioia, L.; Gloaguen, F.; Petillon, F. Y.; Schollhammer, P.; Talarmin, J. *Inorg. Chem.* **2011**, *50*, 12575−12585.
(42) Chouffai, D.; Zampella, G.; Capon, J.-F.; De Gioia, L.; Goff, A. L.; Petillon, F. Y.; Schollhammer, P.; Talarmin, J. *Organometallics* **2012**, *31*, 1082−1091.
(43) Eldredge, P. A.; Bos, K. S.; Barber, D. E.; Bryan, R. F.; Sinn, E.; Rheingold, A.; Averillm, B. A. *Inorg. Chem.* **1991**, *30*, 2365−2375.
(44) Cahill, J. P.; Bohnen, F. M.; Goddard, R.; Krüger, C.; Guiry, P. J. *Tetrahedron: Asymmetry* **1998**, *9*, 3831−3839.
(45) Bras, J. L.; Jiao, H.; Meyer, W. E.; Hampel, F.; Gladysz, J. A. *J. Organomet. Chem.* **2000**, *616*, 54−66.
(46) *Software Packages SMART and SAINT*; Siemens Energy & Automation Inc.: Madison, WI, 1996.
(47) Sheldrick, G. M. *SADABS Absorption Correction Program*; University of Göttingen: Göttingen, Germany, 1996.
(48) Sheldrick, G. M. *SHELXTL97 Program for the Refinement of Crystal Structure*; University of Göttingen: Göttingen, Germany, 1997.